有机化学 DOI: 10.6023/cjoc202112012 研究论文
Chinese Journal of Organic Chemistry ARTICLE

一种具有大斯托克斯位移和高光学稳定性的线粒体靶向近红外染料及其细胞成像应用

周红梅 唐永和 卢辉旭 张 倩 林伟英*

(广西大学化学化工学院 广西电化学能源材料重点实验室 广西大学光功能材料与化学生物学研究院 有色金属及材料加工新技术教育部重点实验室 广西有色金属及特色材料加工重点实验室 广西南宁 530004)

摘要 线粒体功能障碍与阿尔茨海默病(AD)、高血压、糖尿病和神经退化性疾病等严重疾病密切相关, 开发可高度靶向线粒体的荧光染料对于研究线粒体的生理功能至关重要. 但市场上的线粒体染料斯托克斯位移很小, 容易受到自吸收效应的影响. 基于线粒体膜电位的特性设计了一种线粒体靶向染料, 命名为 **Mito-ql**. 染料 **Mito-ql** 具有优异的光学特性, 例如大斯托克斯位移(约 165 nm)良好的化学和光稳定性以及低细胞毒性. 此外, 细胞成像实验表明, 染料 **Mito-ql** 具有优异的线粒体定位能力, 不受线粒体膜电位变化的影响.

关键词 大斯托克斯位移; 荧光成像; 线粒体; 荧光染料

A High Photostability Mitochondrial Targeted Near-Infrared Dye with Large Stokes Shift and Cell Imaging Application

Zhou, Hongmei Tang, Yonghe Lu, Huixu Zhang, Qian Lin, Weiying*

(*Guangxi Key Laboratory of Electrochemical Energy Materials*, *Institute of Optical Materials and Chemical Biology*, *MOE Key Laboratory of New Processing Technology for Nonferrous Metals and Materials*, *Guangxi Key Laboratory of Processing for Non-ferrous Metals and Featured Materials*, *School of Chemistry and Chemical Engineering*, *Guangxi University*, *Nanning*, *Guangxi 530004*)

Abstract Mitochondrial dysfunction is closely related to serious diseases such as Alzheimer's disease (AD), hypertension, diabetes and neurodegenerative diseases. The development of a fluorescent dye that can be highly targeted to mitochondria is essential for studying the physiological functions of mitochondria. However, the Stokes shift of the mitochondrial dyes on the market is very small and is easily affected by the self-absorption effect. Herein, a new mitochondria targeted dye was designed, named as **Mito-ql**, based on the properties of mitochondrial membrane potential. The dye **Mito-ql** has excellent optical properties such as large Stokes shift (about 165 nm), good chemical and photo stability, and low cytotoxicity. In addition, the cell imaging experiments demonstrated that the dye **Mito-ql** has excellent mitochondrial localization ability, which is not affected by changes in mitochondrial membrane potential.

Keywords large Stokes shift; fluorescent imaging; mitochondria; fluorescent dye

1 Introduction

Mitochondria, as one of the important organelles of eukaryotic cells, are involved in many physiological activities.[1] Typically, mitochondria transmit information with reactive oxygen generation signal transduction.[2-3] Mitochondria also could induce cell apoptosis by regulating Ca^{2+} ion balance.[4] In addition, under the catalytic action of H^+-adenosine triphosphate (ATP) synthase, mitochondria can produce ATP, which provides energy for the life activities of normal cells. Therefore, mitochondria are often referred to as "the powerhouses of the cell".[5-7] Microenvironmental changes in the mitochondria are having significant impacts on the activity of living cell. Studies have shown that changes of membrane potential, local micro-

* Corresponding author. E-mail: weiyinglin2013@163.com
Received December 6, 2021; revised February 17, 2022; published online March 21, 2022.
Project supported by the National Natural Science Foundation of China (Nos. 21672083, 21877048, 22077048, 22104019), the Natural Science Foundation of Guangxi Province (Nos. 2021GXNSFDA075003, AD21220061, 2019GXNSFBA245068) and the Startup Fund of Guangxi University (No. A3040051003).
国家自然科学基金(Nos. 21672083, 21877048, 22077048, 22104019)、广西省自然科学基金(Nos. 2021GXNSFDA075003, AD21220061, 2019GXNSFBA245068)和广西大学启动基金(No. A3040051003)资助项目.

viscosity, and micropolarity in mitochondria directly affect the production of ATP and the signal *trans*-molecules of reactive oxygen species (ROS), while triggering cell death.[8-9] Mitochondrial dysfunction is closely related to serious diseases such as Alzheimer's disease (AD), hypertension, diabetes, and neurodegenerative diseases.[10-14] As an important place of cellular oxidative stress, mitochondria are one of the main reasons for the aging of cellular/organismal, which can be used as a strategic target for the treatment of diseases such as cancer.[15-16] Therefore, it is of great significance to develop novel dyes that could stably target mitochondria to further investigate changes in the mitochondrial microenvironment.

Compared with traditional technologies, fluorescent imaging methods have become important tools to monitor subtle changes in the micro-environment of cells and organisms.[17-19] The high selectivity and sensitivity make fluorescent probes/dyes widely applicable in biological imaging.[20-30] Recent years, mitochondrial fluorescent probes are developing rapidly, with the synthesis of commercial mitochondria dyes [such as Mito-Tracker Green (MTG), Mito-Tracker Orange (MTO), Mito-Tracker Red (MTR), and Mito-Tracker Deep Red (MTDR).[31] However, few stable mitochondria fluorescent probes with large Stokes shifts were developed. Therefore, based on this goal, we are aimed to develop a mitochondrial fluorescent probe with large Stokes shift to reduce background interference during imaging.

Herein a new mitochondria fluorescent dye named **Mito-ql** with large Stokes shifts (165 nm) was developed to reduce the self-absorption effect. Follow-up tests' results showed that it has a good resistance to photobleaching and was not affected by pH and chemical substances in biological micro-environment, which also achieved real-time monitoring of the dynamic changes of the mitochondrial microenvironment. As shown in Scheme 1, the new mitochondria fluorescent dye **Mito-ql** has a greater stokes shifts than commercial mitochondrial dyes, which may lead to numerous applications in the future.

2 Results and discussion

2.1 Design of the dye **Mito-ql**

It is well known that the fluorescent emission of most cyanine dyes lies near the infrared region and has large Stokes shift (more than 50 nm), which makes cyanine dyes have a strong ability to resist background interference.[32-33] Therefore, based on our long-term interest in semi-cyanine dye,[34-35] we developed a new fluorescent dye with large Stokes shift, named as **Mito-ql**. The dye **Mito-ql** was constructed using coumarin as the fluorescent platform and quinoline quaternary ammonium salt to form a novel semi-cyanine dye structure. The dye **Mito-ql** contained a structure with positive nitrogen ions, which could be electrostatically adsorbed by the negative charges on the outer mitochondrial membrane, thus enabling the targeting characteristics of mitochondria. The synthesis route of the dye **Mito-ql** was shown in Scheme 2.

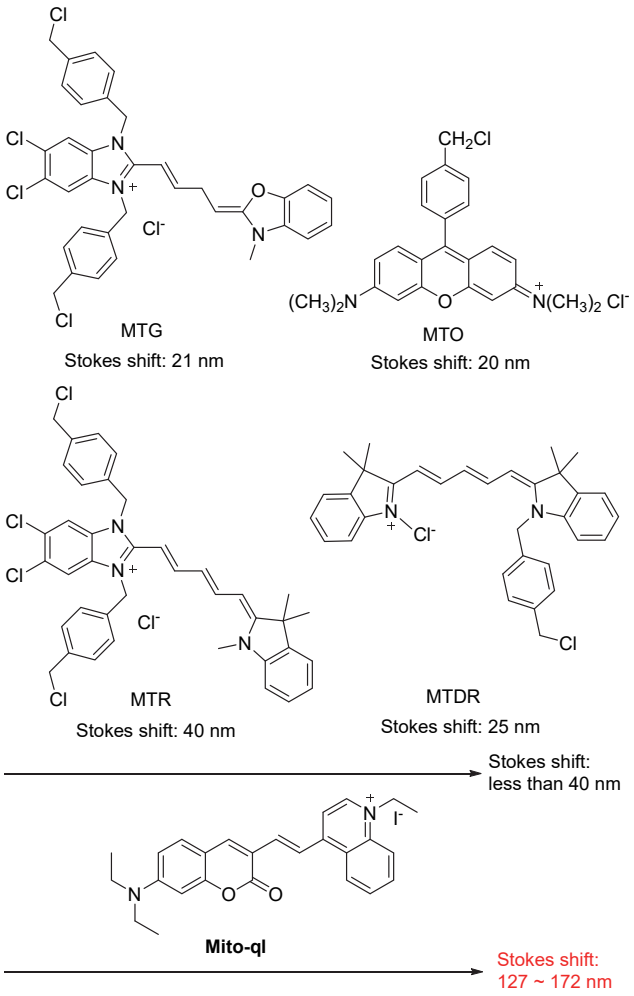

Scheme 1 Stokes shifts and structures of commercial mitochondria dye MTG, MTO, MTR, MTDR and **Mito-ql**

2.2 Spectroscopic properties of **Mito-ql**

The structure of target compound **Mito-ql** was characterized by the NMR and HRMS. In optical property test, the absorption spectra of dye **Mito-ql** (5 μmol/L) was conducted on Shimadzu UV-2700 UV-vis spectrophotometer at room temperature. The absorbance and emission spectra of the dye **Mito-ql** (5 μmol/L) in various solutions (1,4-dioxane, dimethyl sulfoxide (DMSO), acetic acid, acetone, toluene, and EtOH) were shown in Figure 1A and Table 1, the maximum absorption peak of **Mito-ql** occurred in the range of 525～550 nm. The absorption properties of the dye **Mito-ql** in different solvents have little change, showing that the dye has good solvent stability. As shown in the Figure 1B and Table 1, the maximum emission peak of **Mito-ql** emerged in the range of 650～730 nm. The dyes had different emission wavelengths in different solvents, such as 1,4-dioxane, dimethyl sulfoxide, acetic acid, acetone, toluene, and ethanol, and the wavelengths shift red with increasing polarity of the solvent.

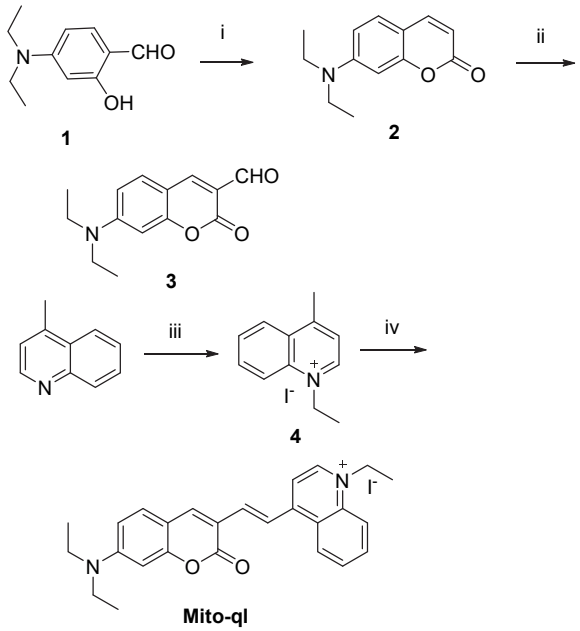

Reagents and conditions: (i) diethylmalonate, piperidine, ethanol, 80 ℃, 6 h; acetic acid and HCl (V∶V=1∶1), 120 ℃, 8 h; (ii) DMF and $POCl_3$ (V∶V=1∶1), 0 ℃, 30 min; Compound **2**, DMF, 60 ℃, 12 h; (iii) iodomethane, 0 ℃, 48 h; (iv) Compound **3**, piperidine, ethanol, reflux, overnight

Scheme 2 Synthesis routes of the dye **Mito-ql**

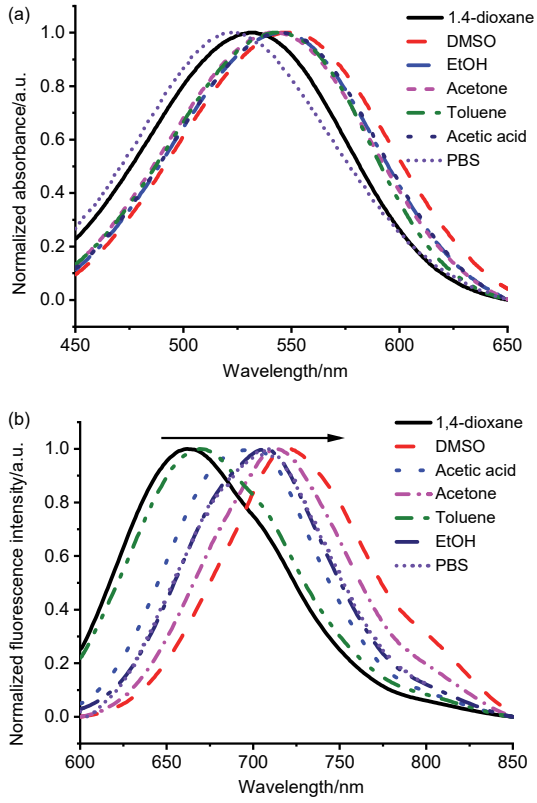

Figure 1 (a) Normalized absorption of **Mito-ql** (5 μmol/L) in different solvents; (b) normalized Fluorescence intensity of the dye **Mito-ql** (5 μmol/L) in different solvents

The Stokes shifts of **Mito-ql** in 1,4-dioxane, DMSO, acetic acid, acetone, toluene, and EtOH had been listed in the Table 1. The quantum yield (Φ) of the dye **Mito-ql** in different organic solvents was also tested. The data of the tests were listed in the Table 1 with the maximum quantum yield reached up to 20%. As a comparison, some optical tests on mitochondrial dyes were also performed. The Stokes shifts of the commercial mitochondrial dyes, such as MTG, MTO, MTR, and MTDR were less than 40 nm in EtOH. In addition, the effect of self-absorption limits to some extent the wide application of these mitochondrial localization dyes. The results demonstrated that **Mito-ql** possessed larger Stokes shift than the commercial mitochondrial dyes, which could effectively avoid the self-quenching effect while providing good imaging conditions for biological applications.

2.3 Chemical and photo stability

As fluorescent tracers, dyes should be chemically and photo stability. Thus, the selective experiment of the dye **Mito-ql** (5 μmol/L) and related bioactive molecules in PBS buffer (10.0 mmol/L, pH 7.40, 20% ethanol as co-solvent) was designed and carried out. As shown in Figure 2, after adding corresponding concentrations of representative anions, metal ions, active oxygen, active nitrogen, reducing agents, RNA, and DNA, the fluorescence intensity hardly

Table 1 Spectroscopic characteristics of **Mito-ql** probe in different solvent

Solvent	ε/(mol•L^{-1}•cm^{-1})	λ_b/λ_a	$\Delta\lambda_s$/nm	Φ_{Fl}/%
Toluene	4.32×10^4	542/669	127	3.09
1,4-Dioxane	4.42×10^4	532/661	129	1.28
Acetic acid	4.84×10^4	545/696	151	19.56
EtOH	4.95×10^4	545/700	165	20.22
Acetone	4.69×10^4	542/712	170	7.96
DMSO	4.34×10^4	549/721	172	13.77
PBS	2.75×10^4	525/703	178	0.25

ε: Molar extinction coefficient; λ_a: extinction maximum; λ_b: emission maximum; Φ_{Fl}: quantum yield of fluorescence.

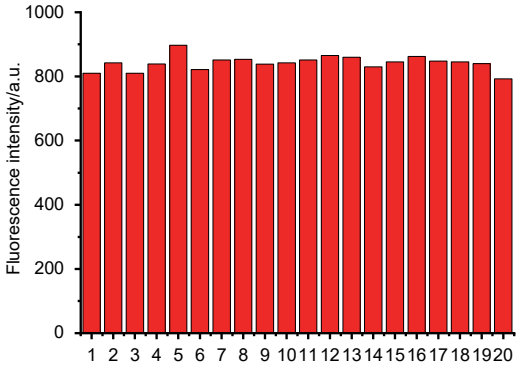

Figure 2 Fluorescence intensities of **Mito-ql** (5 μmol/L) and related ions at λ_{em}=700 nm and related biological species (100 μmol/L)

1, Only probe; 2, AD-glucose; 3, *L*-Arg; 4, *L*-ascorbic acid; 5, Gly; 6, GSH; 7, TBHP; 8, Hcy; 9, Cys; 10, Sodium pyruvate; 11, NO; 12, NaClO; 13, H_2O_2; 14, HCHO; 15, Na_2S; 16, Na_2SO_3; 17, $CaCl_2$; 18, $NaNO_2$; 19, RNA; 20, DNA.

changes, indicating that changes of substances in the micro-environment of the organism would not affect the dye **Mito-ql**. The high selectivity assay of the dye **Mito-ql** indicated strong anti-chemical stability without being affected by the complex composition of substances in living cells.

The cell micro-environmental pH changes would influence the protonation/deprotonation effects of certain groups in the dye, which may lead to changes in fluorescence intensity that are not conducive to the micro-environment in the mitochondria detection. Therefore, as a mitochondrial tracer dye, **Mito-ql** was tested for the change in range of pH 4.01～10.07 on the fluorescence intensity. The data showed that the fluorescence intensity of the dye **Mito-ql** remained stable (Figure 3a), especially in the pH 4～8 physiological range environment (the pH of lysosomes and endosomes is acidic, about 4.7～6.5; the pH value range of cytoplasm and nucleus is neutral, about 7.2～7.4; the pH value range of mitochondria is about alkaline 8.0[36]). The pH interference experiments showed that **Mito-ql** was not affected by pH changes, indicating that the dye was expected to achieve mitochondrial status monitoring in different states.

In addition, photo-stability is one of the important parameters for the preparation of excellent subcellular

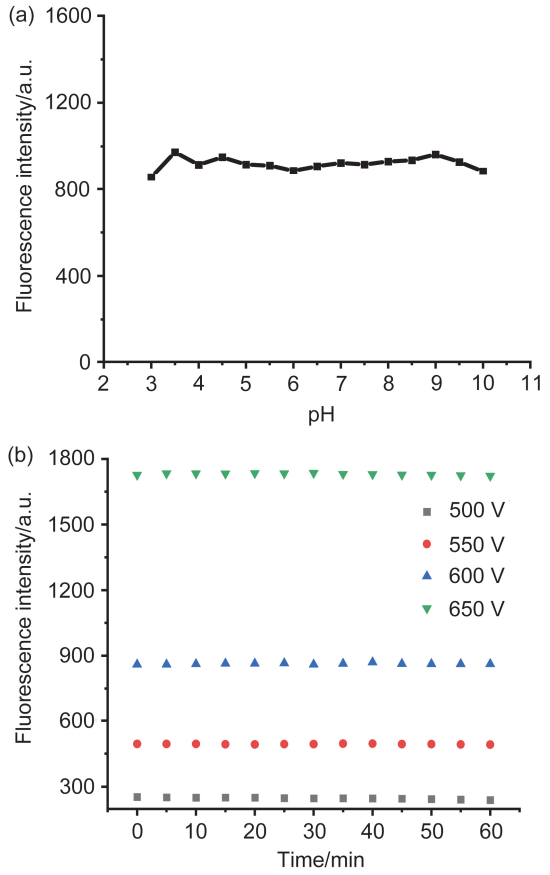

Figure 3 (a) Fluorescence intensity changes of the dye **Mito-ql** (5 μmol/L) at different pH values (3.01～10.07); (b) photostability profiles of the dye **Mito-ql** (5.0 μmol/L) at different voltages (λ_{ex}=550 nm)

structure tracer dye. Therefore, the photo-stability test of dye under at different voltages was investigated. As shown in Figure 3b, the fluorescence intensity of the dye **Mito-ql** in solution hardly changed after 60 min of UV radiation, showing that the dye **Mito-ql** has great photo-stability property. The photo-stability experiments showed that the dye **Mito-ql** could be used to observe cells for a long time under intense laser irradiation.

In summary, the dye **Mito-ql** has near-infrared fluorescence emission, which could effectively avoid the influence of background cell fluorescence. The large Stokes shift of the dye **Mito-ql** could effectively reduce the self-absorption effect. Moreover, **Mito-ql** has significant photo-stability property, good chemical stability, and a wide pH working range. These excellent optical properties motivate us to do subsequent biological imaging applications.

2.4 Confocal fluorescence imaging of the dye **Mito-ql** in living cells

As a biological dye, the dye **Mito-ql** should have low biological toxicity. The data of the **MTT** assays showed that **Mito-ql** has low toxicity and is suitable for biological imaging. After confirming that the dye had good biocompatibility, we began to conduct subsequent cell imaging experiments.

As a mitochondrial organelle tracer dye, **Mito-ql** should have the ability to specifically target mitochondria. The cell co-location imaging experiments were performed to verify the enrichment ability of **Mito-ql** in cellular mitochondria. The living HeLa cells were incubated with commercially available Mito-Tracker Green (MTG), Lys-Tracker Green (LTG), ER-Tracker Blue (ETB) and nucleus blue dye Hoechst 33342 (Hoechst) for 30 min, respectively. Then, the dye **Mito-ql** was added to pre-incubate for another 30 min. After being washed twice with PBS buffer solution and replaced with fresh DMEM medium, the stained HeLa cells were used for confocal imaging by laser scanning confocal microscope. As shown in Figure 4, the HeLa cells showed significant fluorescence in red channel after incubated with **Mito-ql**. At the same time, strong fluorescence signal was observed due to the presence of the commercially available dyes. After comparing, the merged image of **Mito-ql** and MTG could be highly overlapped. In addition, the co-localization imaging of probes in 7702 cells and mouse mononuclear macrophage leukemia cells (RAW cells) were also performed. As shown in Figure 5, the Pearson coefficient in 7702 cells was 85.06% and in RAW cells was as high as 90.58%. These results could show that **Mito-ql** has a specific targeting function to mitochondria and has the potential to detect changes in the mitochondrial micro-environment.

Photo-stability is one of the important factors for the construction of new fluorescent dyes and one of the requirements for long-term observation of organelle state changes in cells. To verify whether **Mito-ql** has good photo-stability in complex cell environment and whether

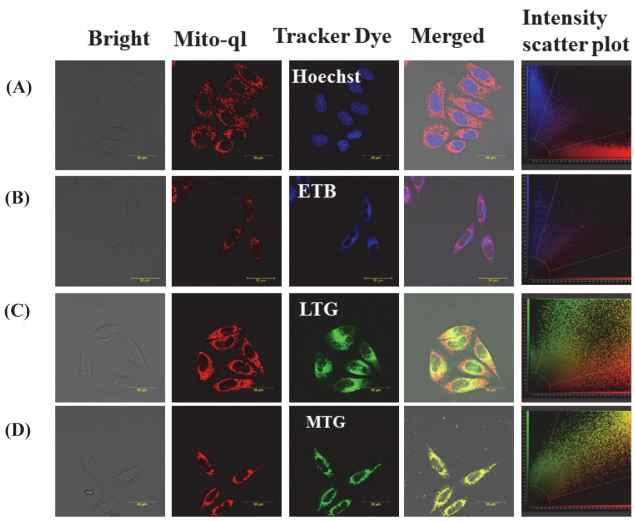

Figure 4 Colocalization of the dye **Mito-ql** (200 nmol/L) and commercial organelle tracker dyes in HeLa cells

(A) The HeLa cells incubated with **Mito-ql** and Hoechst; (B) the HeLa cells incubated with **Mito-ql** and ETB; (C) the HeLa cells incubated with **Mito-ql** and LTG; (D) the HeLa cells incubated with **Mito-ql** and MTG Scale bar=30 μm. λ_{ex}=550 nm, λ_{em}=650～750 nm

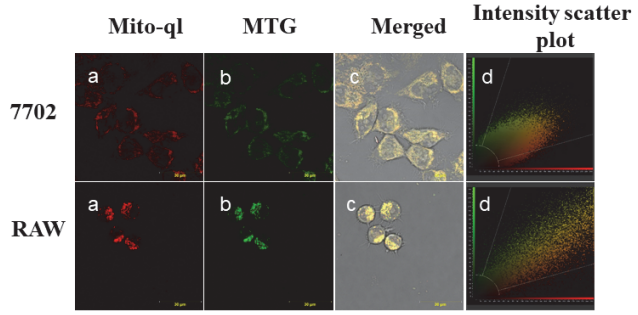

Figure 5 Colocalization of the dye **Mito-ql** (200 nmol/L) and MTG in 7702 cells and RAW cells

Scale bar=30 μm. λ_{ex}=550 nm, λ_{em}=650～750 nm.

Mito-ql could real-time monitor the state of mitochondria in living cells, a group of cell photo-stability imaging experiments was specially designed. The HeLa cells were incubated with **Mito-ql** (200 nmol/L) and imaged by using the confocal microscope with CO_2 incubator at 37 ℃. After the dye **Mito-ql** crossed the cell membrane and entered the cell, the fluorescence intensity of the cell increased rapidly, and the fluorescence growth trend slowed down about 180 s later (Figure 6a). This phenomenon indicated the dye **Mito-ql** has good biocompatibility and could enter the living cell quickly. Moreover, it could also be seen in Figure 6b that the fluorescence channel showed strong filamentous structure, indicating that the dye **Mito-ql** may be enriched in the mitochondria of the cell, which is helpful to recognize the rapid change in real-time, monitoring the mitochondria cell. In addition, after long time laser irradiation (within 660 s), the fluorescence intensity of the staining cells showed no photobleaching phenomenon, indicating that the dye **Mito-ql** could stably exist in the mitochondria. The experimental phenomenon indicated that the dye **Mito-ql** has the potential to monitor the changes in the status of mitochondria over a long period of time.

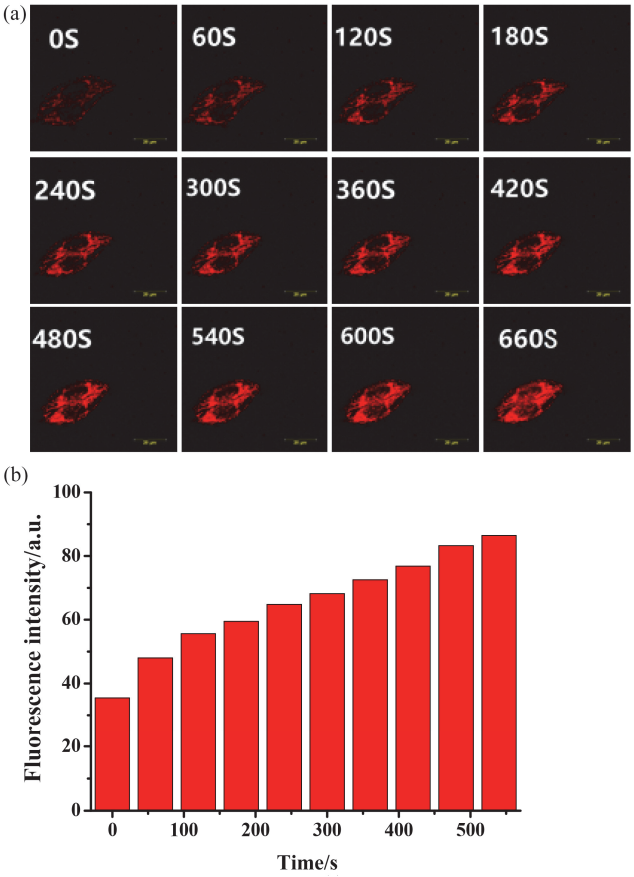

Figure 6 (a) Fluorescence images of HeLa cells incubated with **Mito-ql** acquired at different time; (b) fluorescence intensities of the cells incubated with **Mito-ql** (200 nmol/L) in the red channel at different times

Excitation wavelength: 550 nm, scale bar=30 μm. λ_{ex}=550 nm, λ_{em}=650～750 nm.

To further study the effect of changes in membrane potential on the probe in cell imaging, the mitochondrial membrane potential uncoupling agent carbonyl cyanide 3-chlorophenylhydrazone (CCCP) was used for imaging experiments. CCCP is a kind of H^+ ionophore, which could promote the permeability of mitochondrial intima to H^+, resulting in the loss of membrane potential on both sides of mitochondrial intima and inducing cell apoptosis.[37] The HeLa cells in the experimental group were then incubated with CCCP (10 μmol/L) for 30 min, and washed with PBS buffer solution for three times, while 1 mL of fresh DMEM medium was added and pre-incubated with **Mito-ql** and **MTG** afterwards. As shown in Figure 7, no difference in staining intensity was shown under the conditions of incubation with CCCP, indicating that **Mito-ql** could stably image the mitochondria in the cell in time when the membrane potential is damaged.

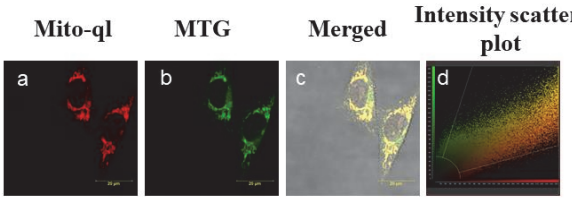

Figure 7 Colocalization of the dye **Mito-ql** (200 nmol/L) and MTG in HeLa cells treated with CCCP

Scale bar=30 μm. λ_{ex}=550 nm, λ_{em}=650～750 nm.

3 Conclusions

In summary, based on traditional coumarin dye, we have constructed a new mitochondrial targeted semi-cyanine dye **Mito-ql** with NIR fluorescence emission and large Stokes shift (127～178 nm in various solutions). The dye **Mito-ql** showed good chemical and photo stability, with low cytotoxicity to living cells while achieving real-time imaging in mitochondria. The fluorescent dye **Mito-ql** with large Stokes shift would provide important information for the study of the distribution and function of mitochondria and changes in the mitochondrial microenvironment.

4 Experimental section

4.1 Instruments and reagents

High resolution mass spectrometric (HRMS) analyses were measured on a Finnigan MAT 95 XP spectrometer. NMR spectra were recorded on an INOVA-400 spectrometer, using TMS as an internal standard. The fluorescence spectra were obtained on a F-4700 spectrofluorometer from Hitachi High-tech Science. The absorption spectra were collected on UV-2700 visible spectrophotometer from Shimadzu Scientific Instruments. The fluorescence imaging of cells was performed with TSC-SP8 (Leica, Wetzler, Germany) confocal laser scanning microscope. The pH measurements were carried out on a PHS-3E PH meter from INESA Instrument. All reagents and materials were purchased from commercial companies and used without further purification unless otherwise stated.

4.2 Materials and methods

The drugs and reagents used in the experiment were purchased from supply stores without further purification. Compounds **3** and **4** were synthesized according to the reported procedures in the literature.[38-39]

4.3 Synthesis of **Mito-ql**

The compound **4** (0.130 g, 0.754 mmol) and piperidine (6 drops) were added into a 100 mL flask, and stirred to dissolve at room temperature. After 10 min, 7-(diethylamino)coumarin-2-carbaldehyde (0.185 g, 0.754 mmol) was added into the previous solution. The mixture was refluxed over the night. Then the reaction solution was vacuum distilled, rotary dried and purified by column chromatography (methanol and dichloride, V∶V=1∶10). For **Mito-ql**: 0.101 g, 45% yield. Dark green solid, m. p. >250 ℃; ^{1}H NMR (600 MHz, $CDCl_3$) δ: 9.63 (d, J=6.5 Hz, 1H), 8.69 (d, J=8.6 Hz, 1H), 8.57 (d, J=15.5 Hz, 1H), 8.47 (d, J=6.5 Hz, 1H), 8.38 (s, 1H), 8.22 (d, J=8.9 Hz, 1H), 8.10～8.03 (m, 1H), 7.95 (d, J=15.5 Hz, 1H), 7.88～7.79 (m, 1H), 7.53 (d, J=8.9 Hz, 1H), 6.64 (d, J=10.7 Hz, 1H), 6.46 (s, 1H), 5.12 (q, J=7.3 Hz, 2H), 3.47 (q, J=7.1 Hz, 4H), 1.75 (t, J=7.3 Hz, 3H), 1.29～1.25 (m, 6H); ^{13}C NMR (150 MHz, $CDCl_3$) δ: 160.42, 156.85, 154.07, 147.51, 146.46, 140.16, 137.71, 135.07, 131.20, 129.02, 127.11, 119.08, 118.09, 116.42, 110.11, 96.72, 52.81, 45.27, 15.61, 12.57; HRMS calcd for $C_{26}H_{27}N_2O_2$ $[M]^+$ 399.2067, found 399.2064.

4.4 Preparation of solutions of probe **Mito-ql** and analytes

2.1 mg of probe was dissolved in 4 mL of DMSO to prepare a stock solution. The selective experiment of the dye **Mito-ql** (5 μmol/L) and related bioactive molecules in PBS buffer (10.0 mmol/L, pH 7.40, 20% ethanol as co-solvent) was designed and carried out. The fluorescence emission spectrums were recorded with a HITACHI F4700 fluorescence spectrophotometer. The excitation wavelength was 550 nm, the excitation slit widths were 10 nm, and the emission slit widths were 10 nm.

Supporting Information Cell culture and cell cytotoxicity assays; preparation of cells stimulated by external sources for imaging experiments; the absorption and fluorescence intensity of probe **Mito-ql**; NMR spectrum and HR-MS (ESI) spectrum of **Mito-ql**; The Supporting Information associated with this article can be found in the online version at http: //sioc-journal.cn/.

References

[1] Finkel, T. *Nature* **2006**, *444*, 151.
[2] Murfin, L. C.; Weber, M.; Park, S. J.; Kim, W. T.; Lopez-Alled, C. M.; McMullin, C. L.; Pradaux-Caggiano, F.; Lyall, C. L.; Kociok-Kohn, G.; Wenk, J.; Bull, S. D.; Yoon, J.; Kim, H. M.; James, T. D.; Lewis, S. E. *J. Am. Chem. Soc.* **2019**, *141*, 19389.
[3] Park, S. H.; Shin, I.; Kim, Y. H. *Anal. Chem*. **2020**, *92*, 12116.
[4] Magi, S.; Piccirillo, S.; Preziuso, A.; Amoroso, S.; Lariccia, V. *Cell Calcium* **2020**, *86*, 102162.
[5] Nakamura, Y.; Park, J. H.; Hayakawa, K. *Exp. Neurol.* **2020**, *324*, 113114.
[6] Scantland, S.; Tessaro, I.; Macabelli, C. H.; Macaulay, A. D.; Cagnone, G.; Fournier, E.; Luciano, A. M.; Robert, C. *Biol. Reprod.* **2014**, *91*, 75.
[7] Zhang, Y.; Cui, P.; Li, Y.; Feng, G.; Tong, M.; Guo, L.; Li, T.; Liu, L.; Li, W.; Zhou, Q. *FASEB J.* **2018**, *32*, 1891.
[8] Li, J.; Wu, D. D.; Zhang, J. X.; Wang, J.; Ma, J. J.; Hu, X.; Dong, W. G. *World J. Gastroenterol*. **2018**, *24*, 1901.
[9] Druck, T.; Cheung, D. G.; Park, D.; Trapasso, F.; Pichiorri, F.; Gaspari, M.; Palumbo, T.; Aqeilan, R. I.; Gaudio, E.; Okumura, H.; Iuliano, R.; Raso, C.; Green, K.; Huebner, K.; Croce, C. M. *Cell Death Dis.* **2019**, *10*, 1.
[10] Gorman, G. S.; Chinnery, P. F.; DiMauro, S.; Hirano, M.; Koga, Y.; McFarland, R.; Suomalainen, A.; Thorburn, D. R.; Zeviani, M.; Turnbull, D. M. *Nat. Rev. Dis. Primers* **2016**, *2*, 1.
[11] Singhal, N. K.; Alkhayer, K.; Shelestak, J.; Clements, R.; Freeman, E.; McDonough, J. *Mol. Neurobiol*. **2018**, *55*, 8051.
[12] Kawamata, H.; Manfredi, G. *Mech. Ageing Dev.* **2010**, *131*, 517.

[13] Malhi, S. S.; Murthy, R. S. R. *Expert Opin. Drug Delivery* **2012**, *9*, 909.
[14] Fan, L.; Zan, Q.; Wang, X. D.; Wang, S. H.; Zhang, Y. W.; Dong, W. J.; Shuang, S. M.; Dong, C. *Chin. J. Chem.* **2021**, *39*, 1303.
[15] Pokorn, J.; Kobilková, J.; Jandová, A.; Vrba, J. *Prague Med. Rep.* **2014**, *115*, 104.
[16] Missiroli, S.; Perrone, M.; Genovese, I.; Pinton, P.; Giorgi, C. *EBioMedicine* **2020**, *59*, 102943.
[17] Liu, M. J.; Ren, X. L.; Meng, X. W.; Li, H. B. *Chin. J. Chem*. **2021**, *39*, 473.
[18] He, L. W.; Yang, X. L.; Ren, M. G.; Kong, X. Q.; Liu, Y.; Lin, W. Y. *Chem. Commun*. **2016**, *52*, 9582.
[19] Zheng, K. B.; Lin, W. Y.; Tan, L. *Org. Biomol. Chem.* **2012**, *10*, 9683
[20] Stephens, D. J.; Allan, V. J. *Science* **2003**, *300*, 82.
[21] Sang, R.-Y.; Xu, X.-P.; Wang, Q.; Fan, Q.-L.; Huang, W. *Acta Chim. Sinica* **2020**, *78*, 901 (in Chinese).
(桑若愚，许兴鹏，王其，范曲立，黄维，化学学报，**2020**，*78*，901.)
[22] Yue, Y.; Huo, F.; Ning, P.; Zhang, Y.; Chao, J.; Meng, X.; Yin, C. *J. Am. Chem. Soc.* **2017**, *139*, 3181.
[23] Dong, B.; Song, X.; Kong, X.; Wang, C.; Tang, Y. H.; Liu, Y.; Lin, W. Y. *Adv. Mater.* **2016**, *39*, 8755.
[24] Gujrati, V.; Mishra, A.; Ntziachristos, V. *Chem. Commun.* **2017**, *53*, 4653.
[25] Hua, C.; Dong, B.; Tang, Y.; Lin, W. *Acc. Chem. Res.* **2017**, *50*, 1410.
[26] Koide, Y.; Urano, Y.; Kenmoku, S.; Kojima, H.; Nagano, T. *J. Am. Chem. Soc.* **2007**, *129*, 10324.
[27] Cheng, D.; Pan, Y.; Wang, L.; Zeng, Z.; Yuan, L.; Zhang, X.; Chang, Y. *J. Am. Chem. Soc.* **2017**, *139*, 285.
[28] Zheng, X.; Xu, L. *Chem. Inform.* **2016**, *52*, 1094.
[29] Yang, Z.-G.; Xiong, J.; Zhang, W.; Li, W.; Pan, W.-H.; Zhang, J.-G.; Gu, Z.-Y.; Huang, M.-N.; Qu, J.-L. *Acta Chim. Sinica* **2020**, *78*, 130 (in Chinese).
(杨志刚，熊佳，张炜，李文，潘文慧，张建国，顾振宇，黄美娜，屈军乐，化学学报. **2020**，*78*，130.)
[30] Minamikawa, T.; Sriratana, A.; Williams, D. A.; Bowser, D. N.; Hill, J. S.; Nagley, P. *J. Am. Chem. Soc.* **1999**, *112*, 2419.
[31] Wang, J. L.; Lin, W. Y. *Biomaterials* **2013**, *34*, 7429.
[32] Gopika, G. S.; HariPrasad, P. M.; Lekshmi, A. G.; Lekshmypriya, S.; Sreesaila, S.; Arunima, C.; Kumar, M. S.; Anil, A.; Sreekumar, A.; Pilla, Z. S. *Mater. Today*: *Proc.* **2021**, *46*, 3102.
[33] Shindy. H. A. *Dyes Pigm.* **2017**, *145*, 505.
[34] He, L.; Yang, X.; Xu, K.; Kong, X.; Lin, W. *Chem. Sci.* **2017**, *8*, 6257.
[35] Li, X.; Long, C.; Cui, Y.; Tao, F. R.; Yu, X.; Lin, W. *ACS Sens*. **2021**, *6*, 1595.
[36] Li, K.; Li, L. L.; Zhou, Q.; Yu, K. K.; Kim, J. S.; Yu, X. Q. *Coord. Chem. Rev.* **2019**, *388*, 310.
[37] Bionda, C.; Portoukalian, J.; Schmitt, D. *Biochem. J.* **2004**, *382*, 527.
[38] Aliaga, M. E.; Gazitua, M.; Rojas-Bolaños, A.; Fuentes-Estrada, M.; Durango, D.; GarcíaBeltrán, O. *Spectrochim. Acta*, *Part A* **2020**, *224*, 117372.
[39] Xiang, M.; Huang, H.; Liu, X.; Tong, Z.; Zhang, C.; Wang, F.; Yu, R.; Jiang, J. *Anal. Chem.* **2019**, *91*, 5489.

(Cheng, F.)

